Robust Control Assignment 1

Report

SC42145: Robust Control
Group 12

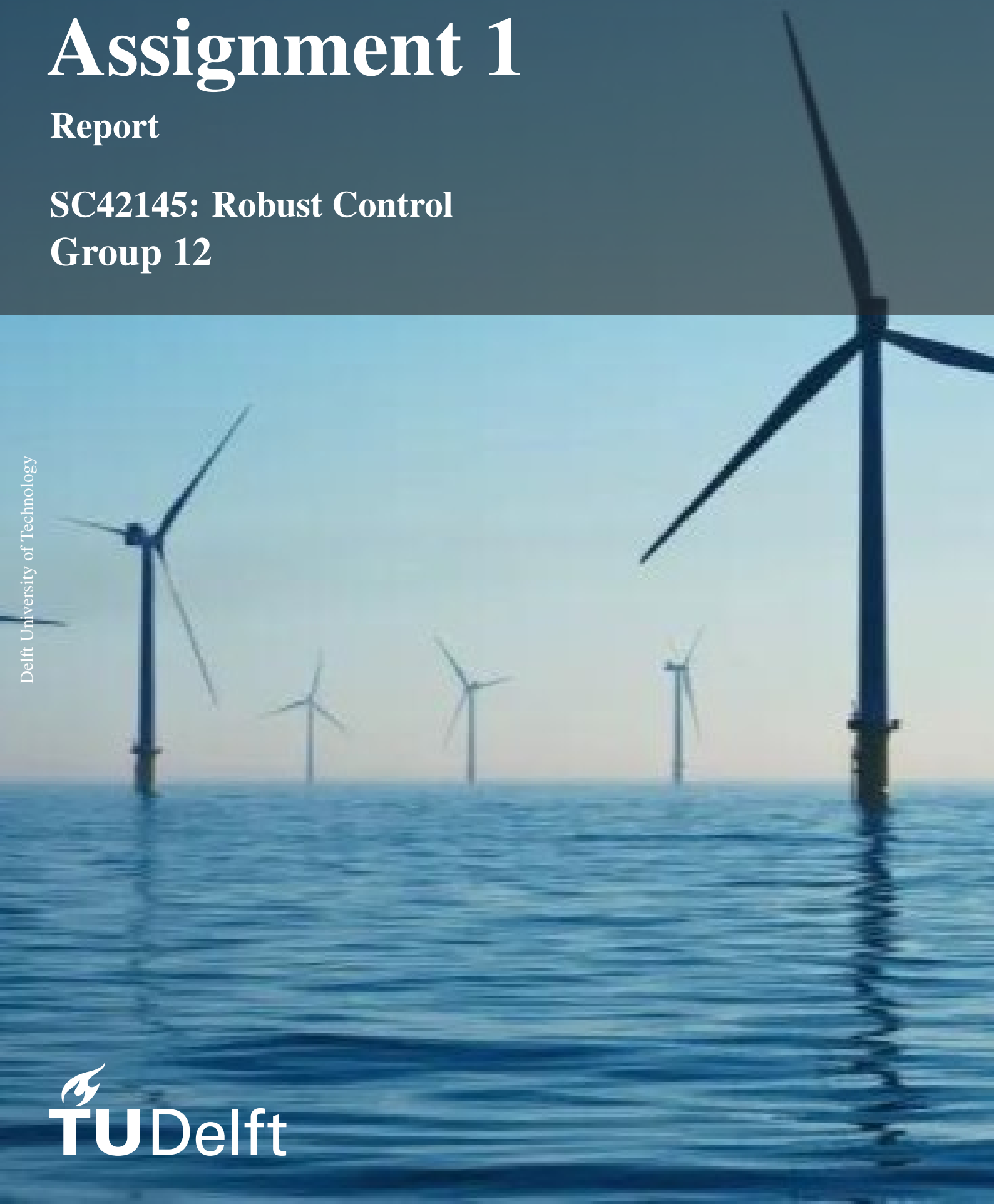

Delft University of Technology

TU Delft

Robust Control Assignment 1

Report

by

Group 12

Student Name	Initials	Student Number
Zoltan Túri	Z.	5213762
Mihaly Fey	M.	5476747

Tutors:
Coaches:
Teaching Assistant: Ing.
Project Duration: - , 2024
Faculty: Systems & Control, Delft

Contents

1. Introduction

The following assignment aims to provide three different controllers designed by different approaches for a floating wind turbine. The states, inputs and outputs of the system are shown in Equation 1.1, whiles the state space matrices are depicted by Equation 1.2 and 1.3. Here ω is the turbine rotational speed, z_1 and z_2 are the displacement components of the end of the windturbine. While the inputs are the blade pitch (β) , generator torque (τ) and wind speed (v_w), it is desired that only the blade pitch is explicitly controlled. The state matrices are obtained by militarization of the nonlinear model about a working point corresponding to 14 m/s.

$$x = \begin{bmatrix} \omega & \dot{z}_1 & z_1 & \dot{z}_2 & z_2 \end{bmatrix}^T \qquad u = \begin{bmatrix} \beta & \tau & v_w \end{bmatrix}^T \qquad y = \begin{bmatrix} \omega & z \end{bmatrix}^T \tag{1.1}$$

$$A = \begin{bmatrix} -0.4220 & -0.2204 & 0 & -0.2204 & 0 \\ 0.0233 & -0.0109 & -0.0400 & -0.0096 & 0 \\ 0 & 1 & 0 & 0 & 0 \\ 0.1455 & -0.0598 & 0 & -0.1651 & -10.8232 \\ 0 & 0 & 0 & 1 & 0 \end{bmatrix} \quad B = \begin{bmatrix} -0.0799 & -0.0096 & 0.2204 \\ -0.0067 & 0 & 0.0096 \\ 0 & 0 & 0 \\ -0.0420 & 0 & 0.0598 \\ 0 & 0 & 0 \end{bmatrix} \tag{1.2}$$

$$C = \begin{bmatrix} 1 & 0 & 0 & 0 & 0 \\ 0 & 0 & 1 & 0 & 1 \end{bmatrix} \qquad D = \begin{bmatrix} 0 & 0 & 0 \\ 0 & 0 & 0 \end{bmatrix} \tag{1.3}$$

In the first chapter, a SISO controller is designed only taking into account the blade pitch and the rotational speed. Next, a Mixed Sensitivity design approach was taken to implement a diagonal controller for the MIMO system. Finally, a fixed structure controller was design to achieve a more viable controller design.

2. SISO Analysis and Design

In this chapter, a SISO controller will be designed for the blade pitch (β) input - rotational speed (ω) output. This way, a constant reference output power can be tracked while keeping the torque (τ) constant. Firstly, the requirements of the controller design is shown. Then the open loop system will be analysed to assess all the possible issues that can rise during the design procedure. Finally, the controller design procedure is presented alongside the results.

2.1. Frequency Domain Requirements

For the SISO system controller design, the requirements are given in the time domain. In order to perform the frequency domain design, these requirements have to be approximated with frequency domain metrics. Thus, in the following section, the relationship between these is presented alongside the final frequency domain requirements.

Settling-time

The first requirement of the wind turbine controller is the settling time of the system's step response. Since the requirement does not specify the error band of the settling time, an error band of 2% was taken. To be able to perform a frequency domain design, this requirement has to be translated to a frequency domain property. As the settling time is closely related to the time constant in the frequency domain, it is also related to the cross-over frequency in the frequency domain. No precise relationship can be obtained for a general system, however, for first-order systems, the relationship of Equation 2.1 can be derived [1, p.244]. Therefore, to achieve the least possible settling time, a high cross-over frequency is required.

$$\frac{3}{\omega_c} \leq t_s \leq \frac{10}{\omega_c} \tag{2.1}$$

Overshoot

The next available requirement is posed on the overshoot of the controlled system. Two possibilities are available to translate the overshoot requirement to a frequency domain requirement. Firstly, the maximum amplification is proportional to the overshoot. When the maximum amplification is less than 1.25 experiments show that the system does not exhibit substantial overshoot [1, p.244].

However, a more precise relationship can be drawn using the phase margin from the phase plot. The phase margin can be related to the damping ratio which again can be related to the overshoot of the system. For a phase margin of 30° the damping ratio is approximately $0.2-0.3$. Increasing the margin to 60° the damping ratio also increases to 0.6. Further elevating the phase margin an aperiodic oscillation is reached at around 90°. In conclusion, the relationship $\zeta = \frac{PM}{100}$ can be used as a first approximation during design [1, p.244].

To get an approximate damping ratio value from the requirement of 1% overshoot, the system can be approximated with Equation 2.2. As a result the damping ratio has to be at least 0.92 to meet the requirements, translating to a phase margin around 90° [2].

$$M_p = 100 \cdot e^{\frac{-\pi\zeta}{\sqrt{1-\zeta^2}}} = 1\% \qquad \rightarrow \qquad \zeta \approx 0.92 \tag{2.2}$$

Steady state error

The controller has to track a constant position signal with zero error. Thus, the system has to be a Type 1 system to eliminate the position tracking error. In the bode plot, the type of system can be inspected in the low-frequency magnitude plot. The initial slope of the graph at the low frequencies tells the Type of the system. The initial slope of the magnitude diagram has to be 20 dB/decade to obtain zero step tracking error [1, p.242].

Summary of Requirements

As the frequency domain representations of the time domain requirements have been found they can be summarised. This summary can be found in Table 2.1

Table 2.1: SISO controller requirements

ID	Time domain	Frequency domain
R-SS-1	The 2% settling time shall be minimized.	The cross-over frequency shall be maximized.
R-SS-2	The overshoot shall be less than 1%.	The phase margin shall be approximately 90 °
R-SS-3	The steady state step tracking error shall be zero.	The magnitude diagram shall have an initial slope of 20 dB/decade

2.2. SISO System Analysis

Using Matlab, the transfer functions were obtained from the State Space system. Equation 2.3 shows the transfer function from the blade pitch input to the rotational speed of the wind turbine. Firstly, inspecting the transfer function, it can be seen that the system is fifth-order and Type 0. This can be verified using the bode plot of Figure 2.1a as the low-frequency line is constant at -15 dB. This results in a position reference signal tracking error, meaning that an integral control action is inevitable in the design to obtain zero tracking error. Without calculating the poles and zeros, it can be concluded that the system is closed-loop stable as the phase margin is positive and has a value of 24.2 dB.

Having a glance at the pole-zero map depicted in Figure 2.1b reveals that the dominant poles correspond to a relatively low damping ratio of 0.052 and frequency of 0.203. As a result, it will be challenging to achieve high bandwidth (cross-over frequency) thus low settling time and high phase margin hence low overshoot.

$$G(s) = \frac{\Omega(s)}{\beta(s)} = \frac{0.07988s^4 + 0.003315s^3 + 0.8677s^2 - 0.006493s + 0.03458}{s^5 + 0.5979s^4 + 10.98s^3 + 4.709s^2 + 0.5421s + 0.1827} \tag{2.3}$$

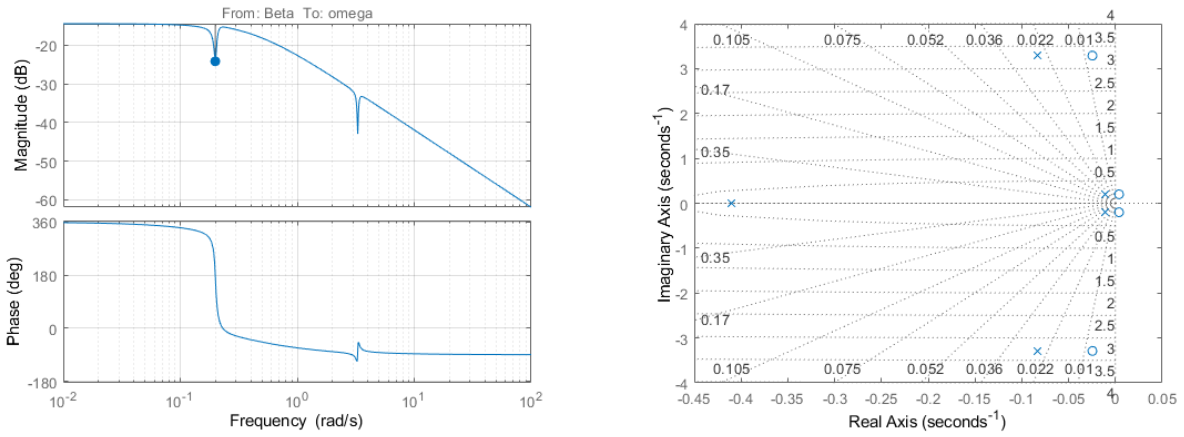

(a) Open loop Bode plot

(b) Pole-zero map of the SISO plant

Figure 2.1: Bode plot and Pole-zero map of the SISO plant

2.3. SISO Controller Design

In the following section the design procedure for the floating wind turbine SISO controller is presented. To achieve the best possible controller design given the set timeframe, two controllers are designed and compared resulting in the most optimal one considering the requirements presented before. A simple feedback structure is selected for both controllers, depicted on Figure 2.2. Finally, the simulation result of the chosen controller is presented.

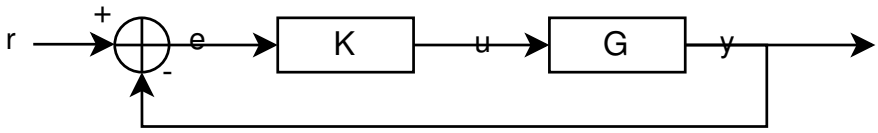

Figure 2.2: Controller architecture of the SISO system

First Design

The first design used the approach provided by the lecture slides. Firstly, the gain was increased to achieve the least possible tracking error while remaining close loop stable. Then, to suppress high-frequency amplification an integral action is applied. This was simultaneously beneficial to the position tracking problem as this way the resultant system is a Type 1 system. Next, a real pole and zero were added to form a lead-lag compensator to create a phase shift, increase the phase margin and meet the overshoot requirement. This step also aided to increase the cross-over frequency and thus, reduce the settling time. Subsequently, a real pole is added to suppress high frequency amplification. Finally, the gain was adjusted to select a cross-over frequency by trading off settle time with the overshoot. The gain was selected so the overshoot requirement was just met while the lowest settling time was achieved. The resultant controller can be seen in Equation 2.4.

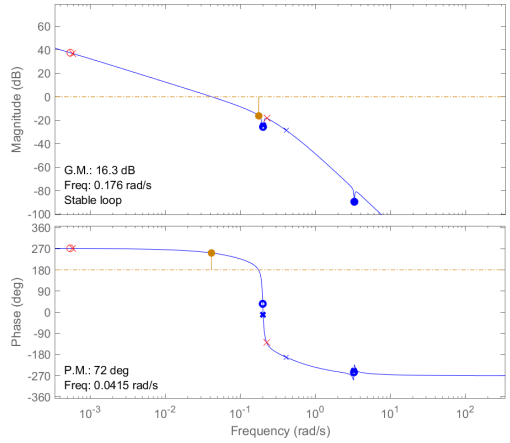

(a) Open loop Bode after designing the first controller

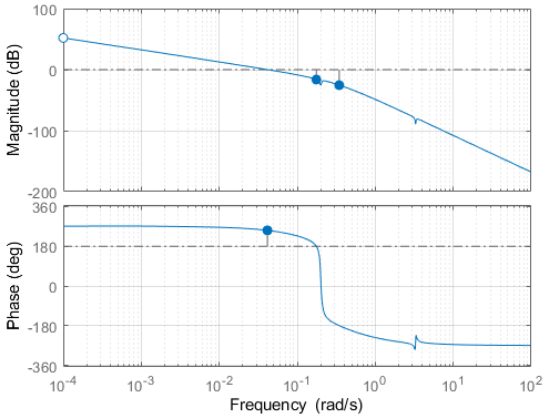

(b) Open loop Bode plot of the first design

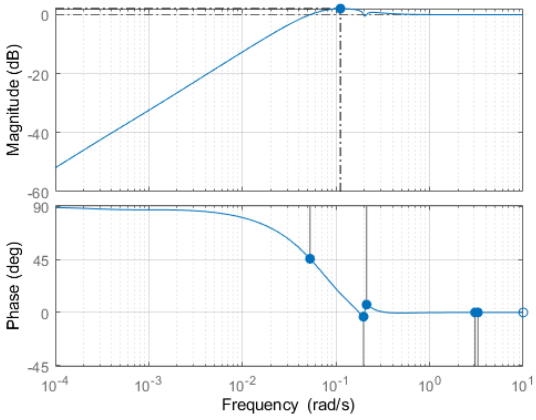

(c) Sensitivity Bode plot of the first design

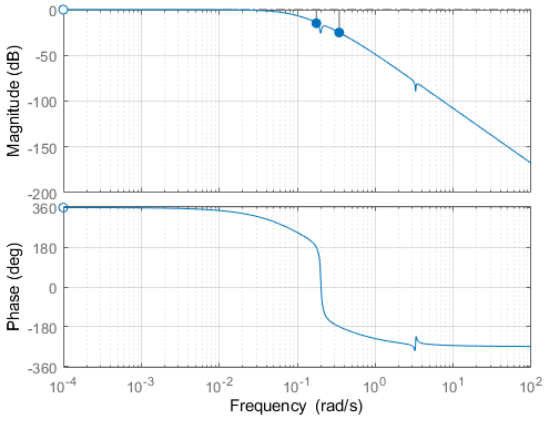

(d) Complementary sensitivity Bode plot of the first design

Figure 2.3: First controller design of the SISO wind turbine system

The results of the initial simulation can be seen in Table 2.2, showing that the requirements are met. The resulting Bode Plots of the design can be seen in Figure 2.3. Figure 2.3a-2.3b show that the controller achieved a Phase Margin of 72°, a Gain Margin of 16.3 dB and a cross-over frequency of 0.0415 rad/s resulting in close-loop stability. This can be verified with the Bode plot of the Complementary Sensitivity transfer function depicted in Figure 2.3d. This plot shows the achieved low-frequency pass behaviour for tracking purposes, while it suppresses the high-frequency noise, such as measurement noise from the sensors. It can be noticed that the achieved Phase Margin is smaller than the estimated required of 90° but the overshoot requirement is still met. This behaviour can be explained by the fact that a second-order system was used to approximate this value which is not a precise approximation for this high-order SISO system.

$$C_1(s) = \frac{0.050425(s+0.0005424)}{s(s+0.2248)(s+0.0005843)} \tag{2.4}$$

Table 2.2: Requirement metrics for the first controller design

Metric	Value	Unit
Settling-time	61.2	s
Overshoot	0.72	%
Steady-state error	0	%
Bandwidth	0.0415	rad/s
Gain Margin	16.3	dB
Phase margin	72	DEG

Second Design

Similarly to the design of the first controller, first the gain was first adjusted to reduce the tracking error. Subsequently, again an integral action was added to eliminate the steady-state step tracking error and suppress low-frequency disturbances. Next, however, a notch filter was added near the complex zero-pole pair of the system increasing the minimum gain margin of the system and depressing high-frequency noise. The resulting controller can be seen in Equation 2.5.

As it can be seen from the Bode plots of Figure 2.4, a higher gain margin of 22.3 dB is achieved compared to the previous design. Contrary, the gain margin has a lower value the before, it is only 69.7°. The H_∞ norm of this design can be read off from the sensitivity Bode plot and has a value of 2.14 dB. The remaining frequency and time domain characteristics of this design can be found in **??**.

$$C_2(s) = \frac{0.15299 \cdot (s^2+0.01552s+0.03945)}{s(s+0.1986)^2} \tag{2.5}$$

Table 2.3: Requirement metrics for the second controller design

Metric	Value	Unit
Settling-time	78.47	s
Overshoot	0.76	%
Steady-state error	0	%
Bandwidth	0.0278	rad/s
Gain Margin	22.3	dB
Phase margin	69.7	DEG

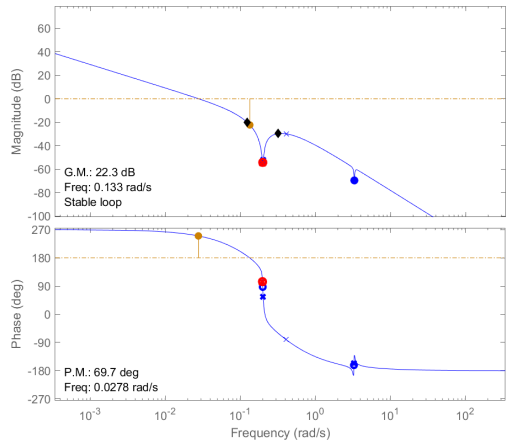

(a) Open loop Bode after designing the second controller

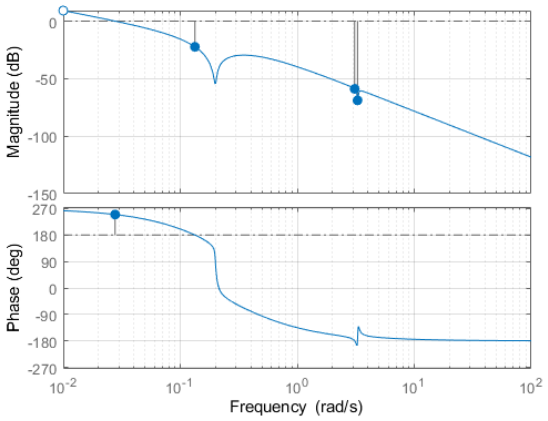

(b) Open loop Bode plot of the second design

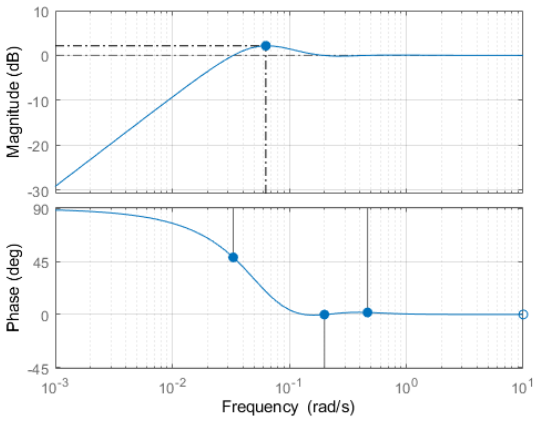

(c) Sensitivity Bode plot of the second design

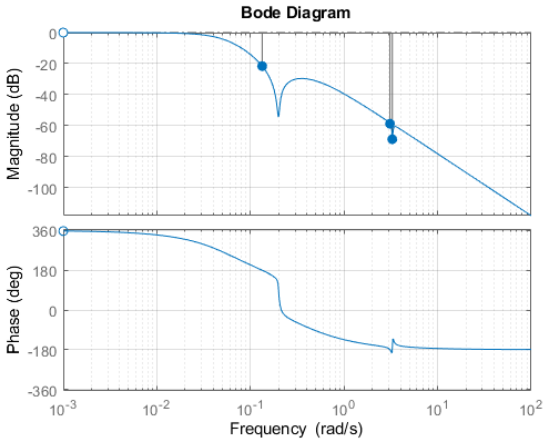

(d) Complementary sensitivity Bode plot of the second design

Figure 2.4: Second controller design of the SISO wind turbine system

Comparison and Controller Selection

As the two controllers have been design so both of them meet the requirements, the better performing shall be selected as the final SISO controller. Since *better performing* is a subjective metric, the design requirements are going to be the decision variables.

Table 2.4: Requirement metrics for the second controller design

Metric	Design 1	Design 2	Unit
Settling-time	61.2	78.47	s
Overshoot	0.72	0.76	%
Steady-state error	0	0	%
Bandwidth	0.0415	0.0278	rad/s
Gain Margin	16.3	22.3	dB
Phase margin	72	69.7	DEG

Figure 2.5a and 2.5b show the step response and step disturbance response of the two designs respectively. Noticeably, both controllers achieve adequate performance in both tracking and disturbance rejection. The first design, however, a higher frequency oscillation in the transient phase in both cases. This behaviour can be concerning for the fatigue wear of the wind turbine structure. On the other hand, the second design

has poorer performance in terms of overshoot and settling time. This is supported by the data contained in Table 2.4. Therefore, the first design is selected as the final controller, as the leading decision parameters are the ones contained in the requirements and the first design outperforms the second one in those.

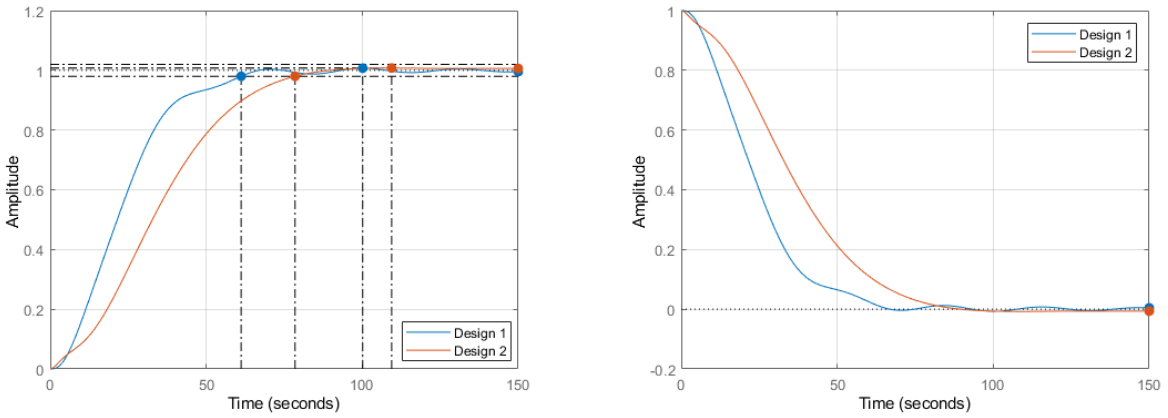

(a) Comparison of the step response of design one and two

(b) Comparison of the step disturbance rejection of design one and two

Figure 2.5: Comparison of design one and two using step response simulations

2.4. Results and Simulations

As the final controller has be selected for the blade pitch SISO controller, the last step remaining is the simulation of the step response and disturbance rejection on the entire system. Figure 2.6 shows the step response with the SISO controller on the complete system. It can be noticed, that as expected, the omega-beta response tracks the reference input flawlessly. However, the other responses have large reference tracking errors. All the out puts, however, are stable. Additionally, Figure 2.7 shows an adequate disturbance rejection on the generator rotational speed output. Finally, Table 2.5 summarizes the performance metrics of the achieved design.

Table 2.5: Requirement metrics for the first controller design

Metric	Value	Unit
Settling-time	61.2	s
Overshoot	0.72	%
Steady-state error	0	%
Bandwidth	0.0415	rad/s
Gain Margin	16.3	dB
Phase margin	72	DEG

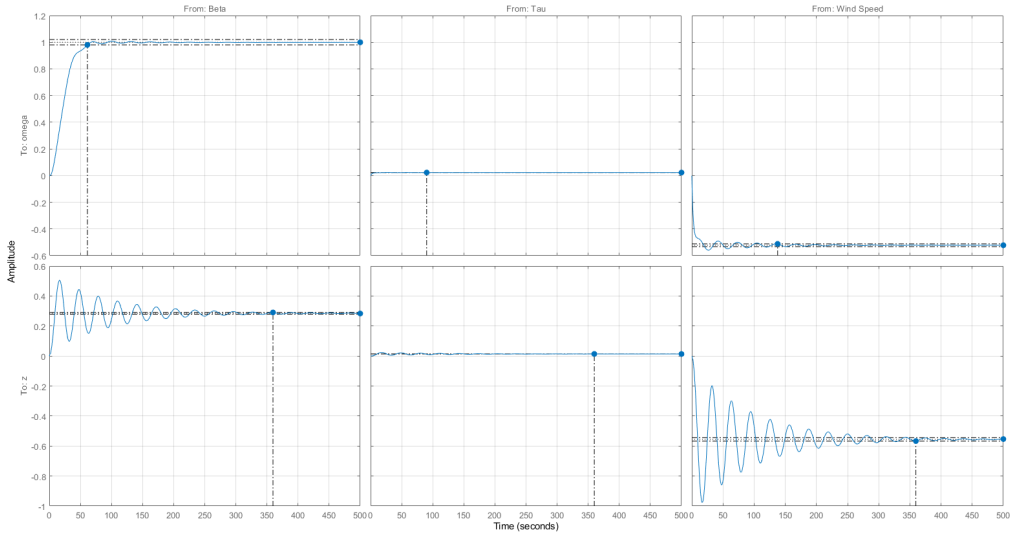

Figure 2.6: SISO controller step response

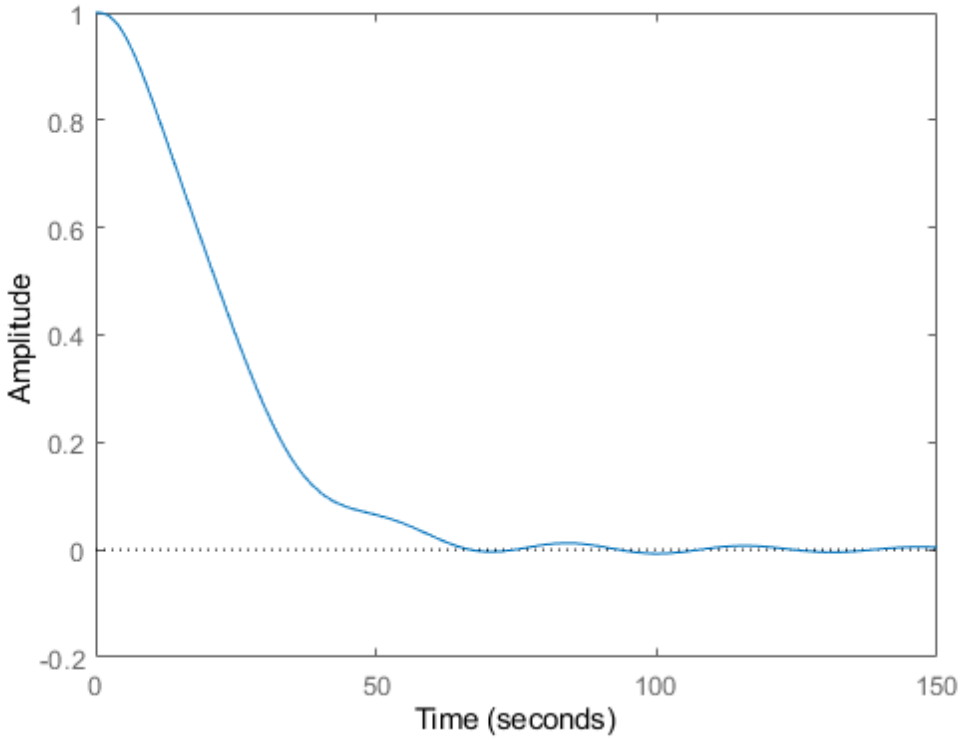

Figure 2.7: Rotational speed disturbance rejection of the SISO controller

3. Multi Variable Mixed-Sensitivity Design

3.1. Frequency Domain Requirements

Contrary to the SISO controller design, here the MIMO controller design requirements are directly given in the frequency domain. Therefore, it is not necessary to transform them between domains.

Table 3.1: Mixed-sensitivity controller requirements

ID	Description
R-MS-1	The cut-off frequency shall be 0.3 Hz.
R-MS-2	The low-frequency attenuation shall be at least 10^{-4}.
R-MS-3	The H-infinity norm of the sensitivity function shall be 3

3.2. MIMO System Analysis

In the following section, the MIMO system will be analysed with the purpose of gaining more knowledge about the stability and controllability of the system. Firstly, the Relative Gain Array (RGA) will be assessed. COnsequently, the pole-zero map is constructed and inspected.

Relative Gain Array

As the first step, the open loop transfer function matrix has to be analysed to investigate the type of controller to be applied to the plant. A simple diagonal controller can only be applied if the states are loosely linked with each other meaning that the system can be decoupled. A good metric to determine the level of interaction between the states is the RGA. For a non-singular square G matrix, the RGA is defined as Equation 3.1, where in the case of a non-square matrix the inverse can be replaced by the pseudoinverse of the matrix.

The relative gain array provides several useful insights to the system. Important to highlight, that the it is dependent on the frequency of the inputs. As it provides important information about the steady state interactions and the interactions at the crossover frequency it is evaluated at angular frequencies 0 rad/s and 0.6π rad/s. The resulting matrices of Equation 3.2 reveal relatively small RGA values. Firstly, the elements of the RGA are relatively small (< 10) in both cases yielding low sensitivity to intup uncertainty, low levels of interactions and thus good controllability. Furthermore, for non-square matrices, the sum of columns provides insight to the necessity of the inputs. As the sum of the elements of the second column corresponding to torque is close to zero this means that the plant can be controlled adequately without this input. This is a desirable property as the torque cannot be controlled directly. Lastly, if the sum of row elements is small ($\ll 1$), the corresponding output is difficult to control. Since this is not the case with the wind turbine plant, all the desired properties are present to be able to design a sufficient diagonal controller. Consequently, a mixed-sensitivity diagonal control indeed can be design and applied for the plant. [3, pp. 87-91]

$$RGA(\omega) = G(\omega) \odot (G(\omega)^{-1})^T \tag{3.1}$$

$$RGA(0) \begin{bmatrix} -2.3694 & 0.0492 & 3.3202 \\ 3.3534 & -0.0254 & -2.3281 \end{bmatrix} \quad RGA(0.6\pi) = \begin{bmatrix} -1.2495 & 0.0283 & 2.2212 \\ 2.2336 & -0.0046 & -1.2290 \end{bmatrix} \tag{3.2}$$

Pole-zero Map

Figure 3.1 shows the pole-zero map of the MIMO plant. It can be seen that the system is stable as all the poles are located on the left half-plane. Again, the dominant poles correspond to a low damping ratio and

natural frequency posing difficulties in meeting the controller requirements. Furthermore, the right half plane poles further slow down the response of the system.

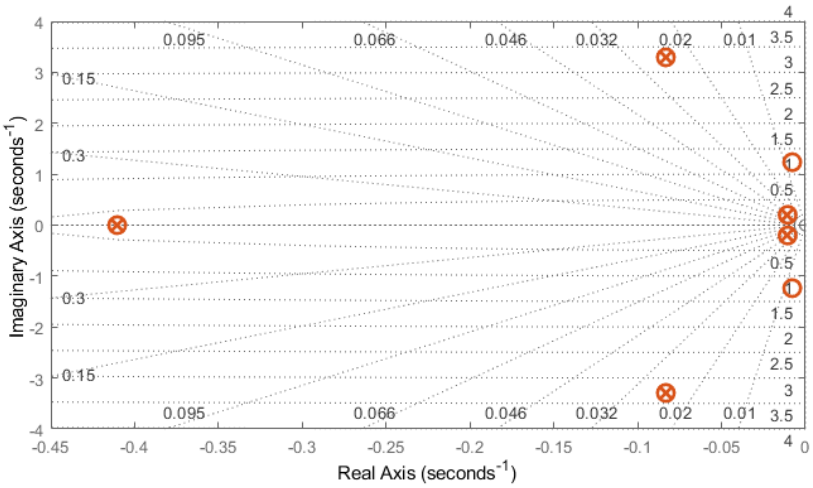

Figure 3.1: Pole-zero map of the floating wind turbine model

3.3. Mixed-Sensitivity Controller Design

In the next design task a step forward was taken from the SISO controller and a diagonal MIMO controller was designed using a Mixed Sensitivity Loop Shaping technique. The procedure for designing such a controller is presented in this section.

The aim of Mixed Sensitivity design is to simultaneously design for reference tracking, disturbance rejection and noise suppression while minimizing the H_∞ norm. To perform this design the controller architecture of Figure 3.2a is assumed. Next weighting functions must be provided, which define the desired shapes of the sensitivity, control effort and complementary sensitivity for the loop shaping. Since the complementary sensitivity is just the complementer set of the sensitivity, in the current design process this output is not used for loopshaping. This assumption modifies the initial block diagram to the one depicted in Figure 3.3a used for the mixed sensitivity design. Here the signals z_1 and z_2 are the performance signals characterizing the disturbance rejection and control effort respectively.

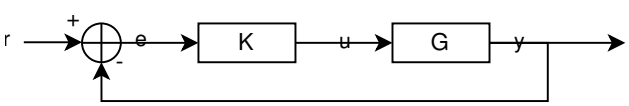

(a) Control architecture of the Mixed Sensitivity design

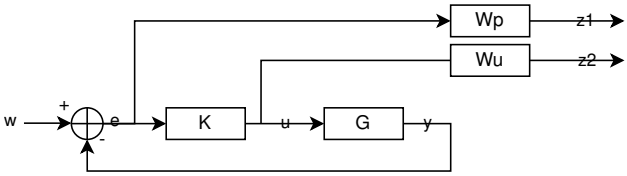

(b) Block diagram appended with the performance weighting blocks

$$||M(s)||_\infty = \left|\left|\begin{bmatrix} W_p S \\ W_2 K S \end{bmatrix}\right|\right|_\infty \leq 1 \qquad (3.3)$$

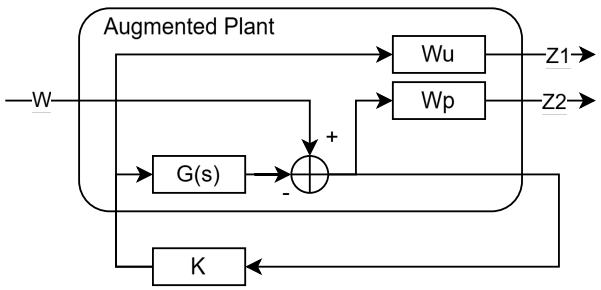

(a) Generalized plant for the Mixed Sensitivity design

After the appropriate shaping functions are selected, the gain, K, is selected to perform the loop shaping using the selected weighting functions and the constraint of Equation 3.3. The augmented plant of the generalized plant can be seen in Figure 3.3a. This augmented plant is utilized for H_∞ minimization. Here w is defined as $[d\ r\ ]$, d being the output disturbance and r being the reference signal. Whilst, z_1 and z_2 are the difference between the output signals and the corresponding reference signal.

Weighting Matrices

As proposed in the assignment, the weighting matrices shown in Equation 3.4 are used to control the MIMO system. It can be seen that the only diagonal element still to be designed is W_{p11}. This weighting element has to be selected such that it has the frequency domain properties that meet the requirements of the sensitivity function. In the Mixed Sensitivity loop shaping, the gain is optimized to achieve a loop shape closest to the inverse of the corresponding weighting function. Therefore, the amplification at low frequencies of W_{p11}^{-1} has to be -60 dB to meet the low-frequency attenuation requirement of 10^{-6}. Furthermore, the bode diagram has to cross the -3 dB line at 3 Hz and the maximum gain has to be $20\log_{10}(3) \approx 9.54$ dB.

$$W_p = \begin{bmatrix} W_{p11} & 0 \\ 0 & 0.05 \end{bmatrix} \qquad W_u = \begin{bmatrix} 0.005 & 0 \\ 0 & \frac{5\cdot10^{-3}s^2+7\cdot10^{-4}s+5\cdot10^{-5}}{s^2+14.10-4s+10^{-6}} \end{bmatrix} \qquad W_{p11}^{-1}(s) = K\frac{s/z+1}{s/p+1} \tag{3.4}$$

As a result, a simple lead-lag transfer function has been used as presented in Equation 3.4, since such transfer function can meet all the requirements without compromise. Using the three requirements, the three equations shown in Equation 3.5 can be written. Solving these equations for K, z and p, the transfer function and weighting function shown in Equation 3.6 is obtained. To verify that the designed weight has the desired loop shape, the corresponding Bode plot is shown in Figure 3.4b. Figure 3.4a shows the Bode plot of the second diagonal element of the control effort. Here, a smaller low-frequency attenuation and cross-over frequency can be seen alongside with a bigger maximum amplification. The Bode plots of the other elements are not presented as they are solely gain elements.

$$|W_{p11}^{-1}(0)| = K = 10^{-4} \qquad \lim_{\omega\to\infty}|W_{p11}^{-1}(\omega i)| = K\frac{p}{Z} = 3 \qquad |W_{p11(0.6\pi i)}^{-1}| = K\left|\frac{0.6\pi i/z+1}{0.6\pi i/p+1}\right| = 10^{-3/20} \tag{3.5}$$

$$W_{p11}^{-1} = 10^{-4}\frac{s/(2.587\cdot10^{-4})+1}{s/7.761+1} = \frac{3s+7.761\cdot10^{-4}}{s+7.761} \qquad \Rightarrow \qquad W_p = \begin{bmatrix} \frac{s+7.761}{3s+7.761\cdot10^{-4}} & 0 \\ 0 & 0.05 \end{bmatrix} \tag{3.6}$$

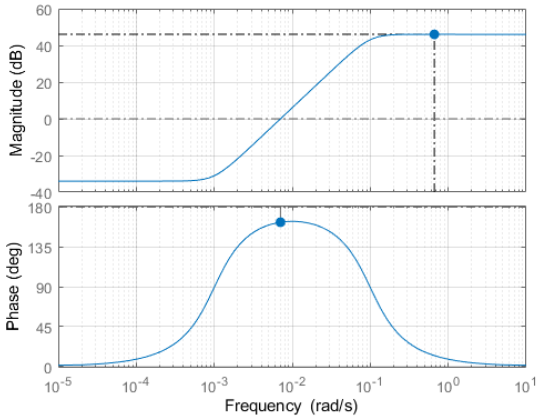

(a) Bode plot of the invers weighting function W_{u22}

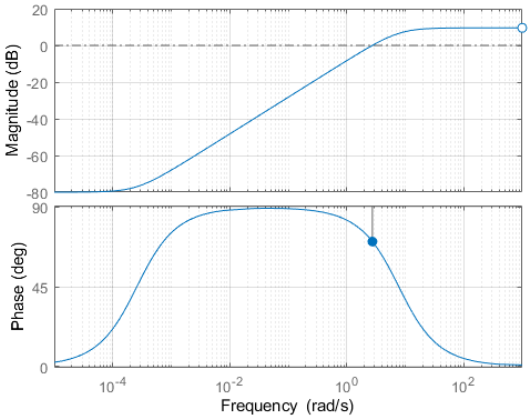

(b) Bode plot of the invers weighting function W_{p11}

Mixed Sensitivity Design

After designing the appropriate weighting functions, the next step is to obtain the optimal gain that optimizes for minimum singular values and closest loop shape to the inverse weighting functions. To perform this optimization, the *hinfsyn* function of Matlab was utilized. The state space form of the resulting controller can be seen in Equation 3.7-3.9.

The effect of the loop shaping is depicted in Figure 3.5. It can be seen that the Sensitivity plots closely approach the target ones. This can also be verified with Figure 3.6, as the singular final values approach the target ones. This figure also shows that the maximum singular value is 0.3357, well below one, meaning that the controller optimization was successful.

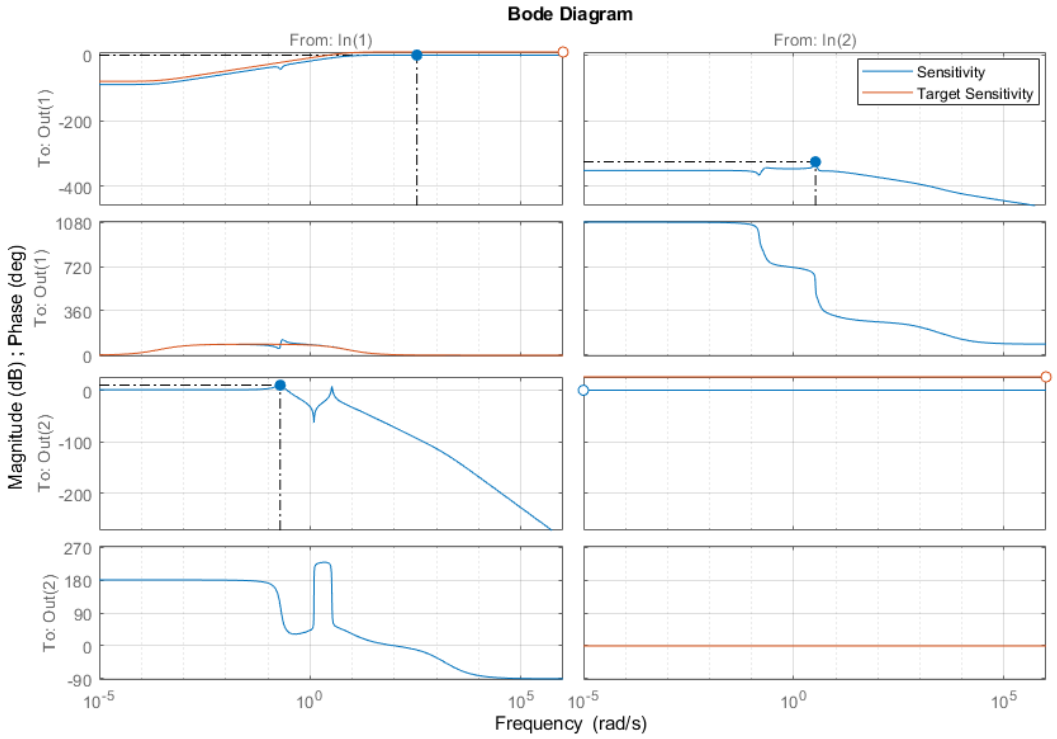

Figure 3.5: Sensitivity Bode plots of the closed-loop system

$$A = \begin{bmatrix} 1470 & 738.6 & 1347 & 1355 & -1169 & 64.61 & -171.7 & 0.2497 \\ -443.1 & -224.2 & -409.6 & -410.5 & 355.1 & -18.32 & 51.95 & -0.07691 \\ -2256 & -1136 & -2067 & -2080 & 1794 & -99.08 & 263.4 & -0.3832 \\ 3378 & 1702 & 3094 & 3114 & -2685 & 148.5 & -394.4 & 0.5736 \\ 3839 & 1932 & 3514 & 3537 & -3050 & 169.8 & -448.2 & 0.6506 \\ -9406 & -4741 & -8616 & -8671 & 7477 & -414.5 & 1098 & -1.596 \\ 3400 & 1713 & 3113 & 3134 & -2702 & 149.9 & -397 & 0.5757 \\ 7.271 & 3.659 & 6.666 & 6.615 & -6.033 & 0.5839 & 0.2578 & 0.002464 \end{bmatrix} \tag{3.7}$$

$$C = \begin{bmatrix} -4.914 & -2.257 & -4.259 & -3.01 & 3.673 & 0.1797 & 0.4983 & -0.001976 \\ -0.164 & -0.05878 & -0.1735 & 0.1988 & 1.147 & -1.062 & -4.408 & -0.01054 \\ 1.466 \cdot 10^4 & 7384 & 1.342 \cdot 10^4 & 1.351 \cdot 10^4 & -1.165 \cdot 10^4 & 645.5 & -1711 & 2.486 \end{bmatrix} \tag{3.8}$$

$$B = \begin{bmatrix} -1.121 & 1.069 \cdot 10^{-15} \\ -0.5803 & 5.412 \cdot 10^{-16} \\ -0.9781 & -1.137 \cdot 10^{-15} \\ -0.9095 & 2.044 \cdot 10^{-16} \\ 0.7786 & 6.326 \cdot 10^{-16} \\ 0.1062 & 7.817 \cdot 10^{-16} \\ 0.07819 & -4.63 \cdot 10^{-18} \\ -0.0003121 & -3.21 \cdot 10^{-17} \end{bmatrix} \qquad D = \begin{bmatrix} 0 & 0 \\ 0 & 0 \\ 0 & 0 \end{bmatrix} \tag{3.9}$$

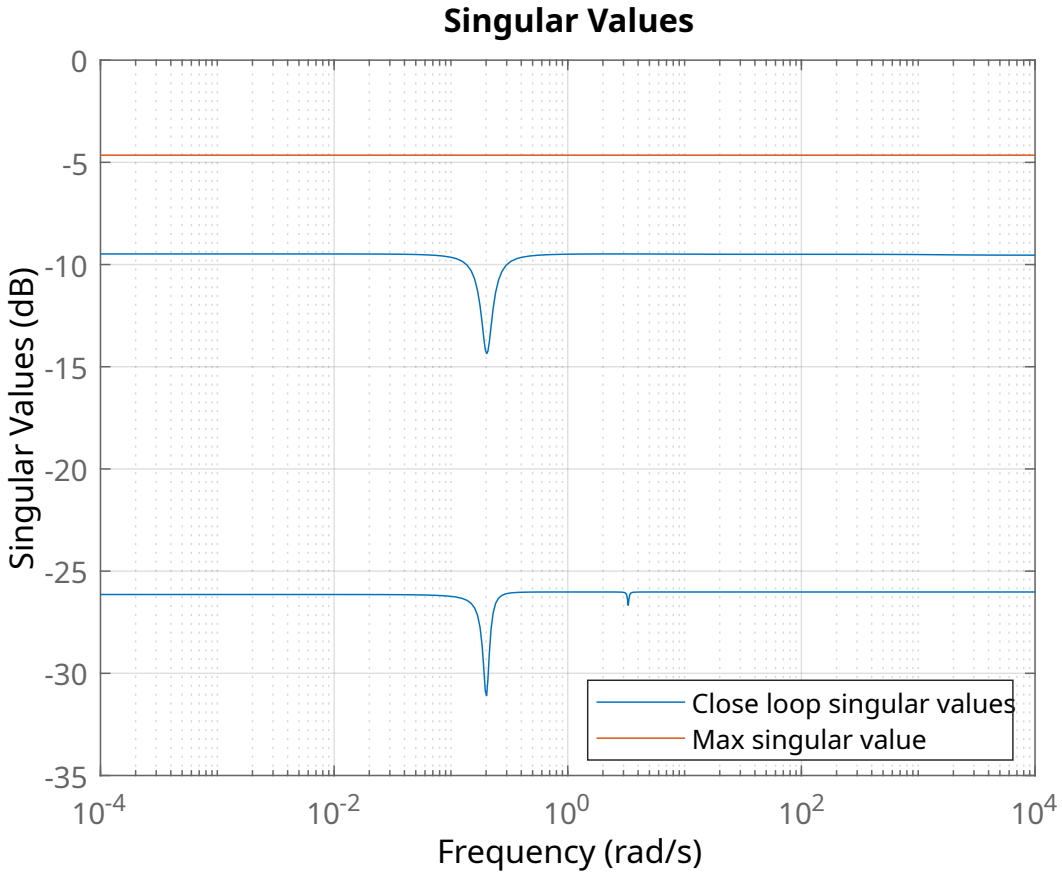

Figure 3.6: Closed loop singular values and maximum singular value

3.4. Results and Simulations

Finally, the last step in the mixed sensitivity controller design is to evaluate the controller using simulation results. In Figure 3.7 and 3.8 the step response and the step disturbance rejection of the system are depicted. Furthermore, Table 3.2 shows the key time and frequency domain properties of the step response. This table also includes the values for the SISO design for comparison. It can be seen that as expected the Mixed Sensitivity design outperforms the SISO controller in all of the metrics.

Table 3.2: Mixed Sensitivity performance metrics

Metric	$\omega_r - \omega$	$\omega_r - z$	SISO
Settling time [s]	0.58	98	61.2
Overshoot [%]	0.67	57	0.72
Steady-state error [%]	0	-	0
Bandwidth [rad/s]	7.76	0.69	0.0415
Gain margin [dB]	Inf	-5.39	16.3
Phase margin [DEG]	89	-6.77	72

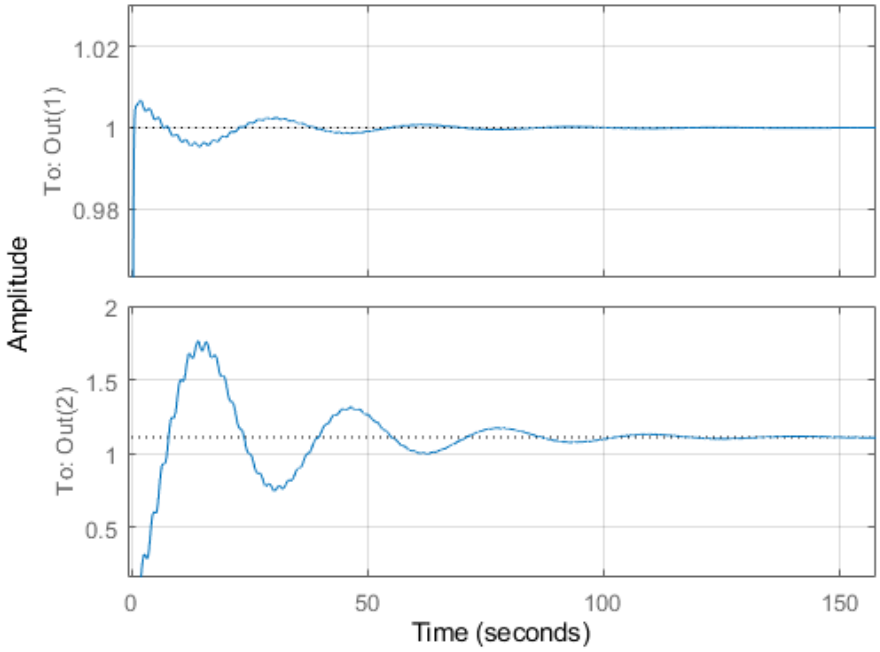

Figure 3.7: Step response with Mixed Sensitivity controller. In(1) is the rotational velocity, whilst Out(1) and Out(2) are the rotational velocity and tower displacement.

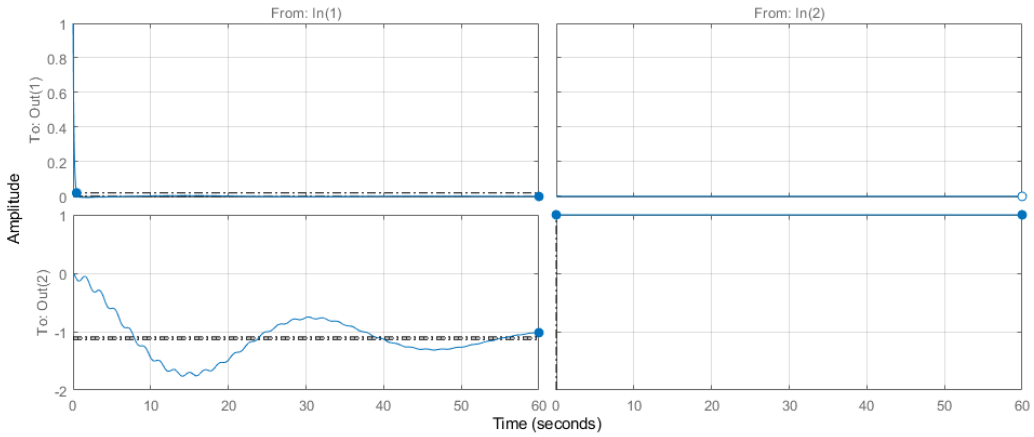

Figure 3.8: Disturbance rejection with Mixed Sensitivity controller. In(1) and In(2) are the disturbances on the output rotational velocity and displacement respectively, whilst Out(1) and Out(2) are the rotational velocity and tower displacement.

4. Fixed-strucutre controller design

4.1. SISO system

The SISO system can be constructed in the same way as in chapter 2, from the A, B, C, D matrices of the wind turbine system. The block diagram with the generalized plant can be seen in Figure 4.1

4.2. Controller structure selection

Since the SISO system is Type 0 and has steady state error an integral term has to be incorporated, so a PI controller was added. Additionally two pole-zero pairs were added, adding a lead-lag (LL) compensator to the system, after the actuation of the PI controller. This gave the controller transfer function in Equation 4.1 and the following list of parameters: Kp, Ki, z_1, z_2, z_2, p_1, p_1, p_2

$$K = \frac{(s-z_1)\cdot(s-z_2)}{(s-p_1)\cdot(s-p_2)}(Kp+\frac{Ki}{s}) \tag{4.1}$$

For reference all design steps were also performed on a reference PID controller, with the transfer function in Equation 4.2 and the following design parameters: Kp, Ki, Kc, Tf.

$$K = Kp+\frac{Ki}{s}+\frac{Kd\cdot s}{Tf\cdot s+1} \tag{4.2}$$

4.3. Controller optimization

The controller parameters were optimized with `hinfstruct`. The example code included 5 random starting positions, as the optimized values of the control coefficients might not be the global optimum with only one starting location. The default value 5 led to very different number between reruns of the program, so this sample size was increased to 50, which still had very inconsistent results. The results of 5x50 runs are in Table 4.1. The run with the lowest settling time was selected, which shows that the PID is not much more performant, on average or it is just less sensitive to the tuning parameters. The final parameter values can be found in Table 4.2.

In either case and irrespective of the values tuning variables the H_{inf} norm of the combined system was 2.6101 after the optimization. The fact that the norm could be 2.61 with a whole host of different parameter values means that just optimizing for the H_{inf} norm of the transfer function does not properly tune this kind of SISO system.

4.4. Performance of the SISO systems

At this point three controllers can be compared to each other, the manual design and the two designed with `hinfstruct`. Their performance was evaluated on a step input to the reference generator speed without wind disturbance and on one with the wind disturbance.

The undisturbed step input can be seen in Figure 4.2. The bad performance metrics in the previous section already suggest that the performance will be sub-par, and it is evident in in the figure.

Table 4.1: Step responses of the PID and LL controller

-	PID controller	Lead-PI controller
Rise time [s]	21.9917	546.0907
Settling time [s]	65.2850	960.6536
Overshoot	2.7070	0

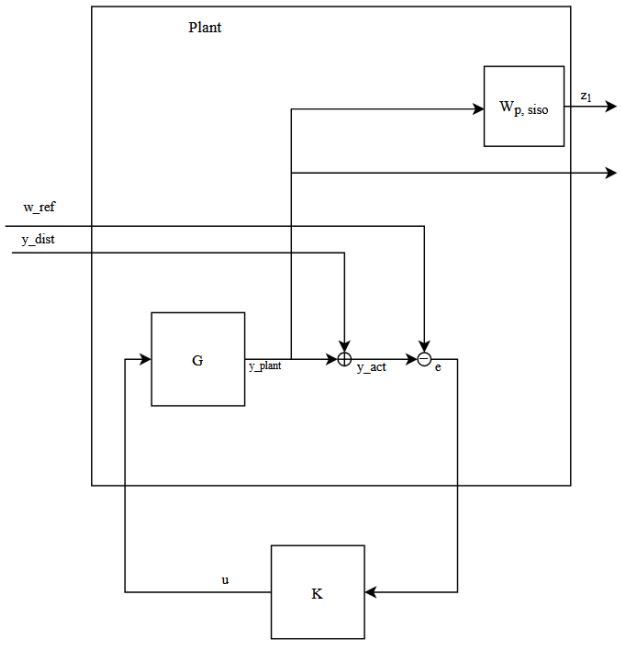

Figure 4.1: Block diagram of the wind turbine with SISO plant model

Table 4.2: Final parameter values

PID controller	LL controller
$Kp = 0.2747$	$Kp = 5.7460$
$Ki = 0.4934$	$Ki = 8.4721$
$Kd = 5.2602$	p_1 = -9.5582
$Tf = 0.1354$	p_2 = -6.5568
-	z_1 = -2.7138
-	z_2 = -0.0612

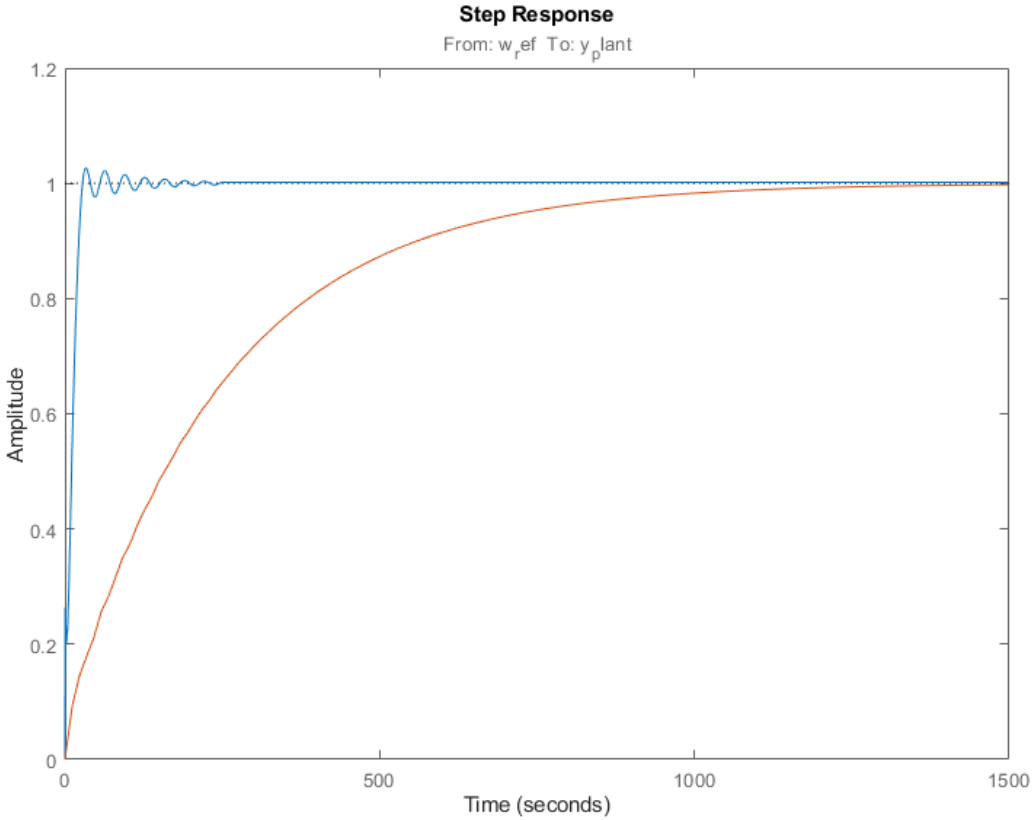

Figure 4.2: Step response of the PID and the LL controllers.

Looking at the disturbance rejection in Figure 4.3 the different behavior of the controllers is also as expected, with the LL controller not being anywhere near the required performance. The PID and the manual controllers are very closely matched; the PID offers a bit faster action but the disturbance rejection is worse due to integrator having the pole at 0. The same can be said about the weighted output.

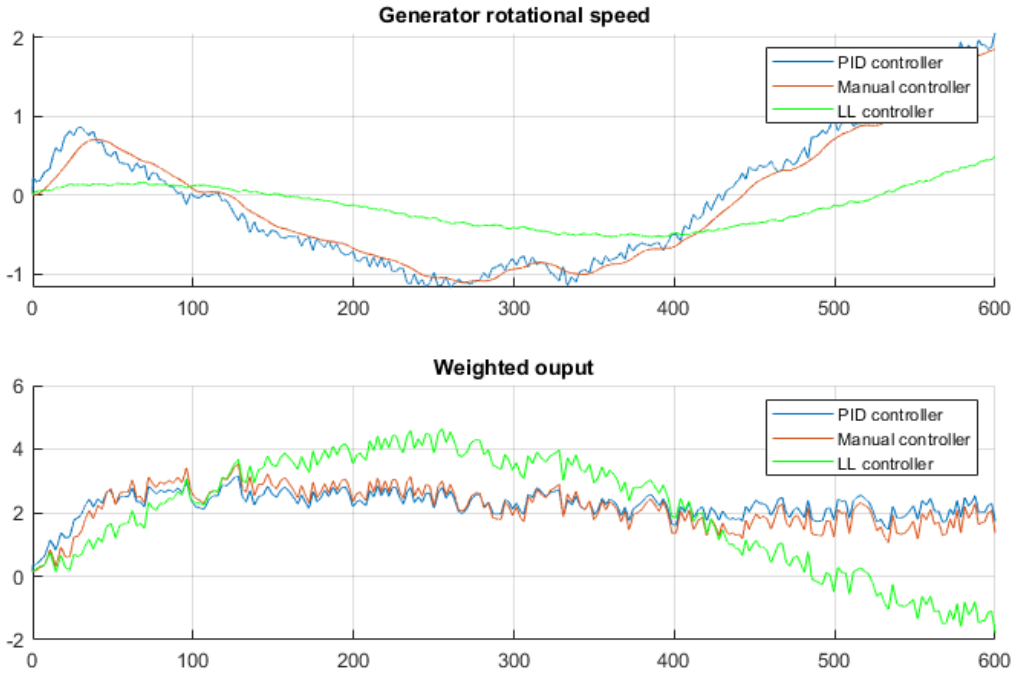

Figure 4.3: Comparison of manual, PID and LL controllers

References

[1] László Keviczky, Ruth Bars, Jenő Hetthéssy et al. *Control Engineering*. Springer Nature Singapore Pte Ltd., 2019. DOI: https://doi.org/10.1007/978-981-10-8297-9.

[2] Gene F. Franklin, J. David Powell and Abbas Emami-Naeini. *Feedback Control of Dynamic Systems*. Pearson Higher Education, 2010.

[3] Sigurd Skogestad and Ian Postlethwaite. *Multivariable Feedback Control Analysis and Design*. John Wiley Sons, 2001.